DOI: 10.1002/ejic.200601003

Effect of Protonation and Interaction with Anions on a Lead(II) Complex with a Lateral Macrobicycle Containing a Phenol Schiff-Base Spacer

David Esteban-Gómez,[a] Carlos Platas-Iglesias,[a] Fernando Avecilla,[a] Andrés de Blas,*[a] and Teresa Rodríguez-Blas*[a]

Keywords: Lead / Macrocycles / N,O ligands / Density functional calculations

The macrobicycle receptor **L⁴**, derived from 1,10-diaza-15-crown-5 incorporating a phenol Schiff-base spacer, forms stable complexes with lead(II). In $[Pb(L^4)(ClO_4)](ClO_4)\cdot CH_3CN$ (**1**), the lead(II) ion is asymmetrically placed at the one end of the macrobicyclic cavity, because of the intramolecular hydrogen bonding interaction that occurs between an imine nitrogen atom and the phenol group. This asymmetric position of the metal ion inside the macrobicyclic cavity induces chirality in this system. Variable temperature ^1H NMR spectroscopic experiments indicate that the asymmetric coordination of the metal ion inside the macrocyclic cavity is maintained in acetonitrile solution, but a translocation of the Pb^{II} ion from one end of the macrobicyclic cavity to the second one occurs. This dynamic behaviour, which corresponds to the interconversion between the two possible enantiomeric forms of the complex, is fast on the NMR timescale at 320 K but slow at low temperatures, and we have estimated an activation barrier of $\Delta G^{\ddagger} = 68 \pm 2$ kJ mol^{-1}. We have also studied the effect of the protonation on **1** by NMR and UV/Vis spectroscopy in CH_3CN solutions at room temperature, finding that diprotonation causes demetallation of the complex without receptor destruction, recovering **L⁴** in its protonated form. On the other hand, the interaction of compound **1** with anions such as NO_3^- and SCN^- has been evaluated by using spectrophotometric titrations in acetonitrile solution, finding log *K* values of 5.83(1) for NO_3^- and 6.27(2) for SCN^-. The $[Pb(L^4)]^{2+}$, $[Pb(L^4)(NO_3)]^+$, $[Pb(L^4)(NCS)]^+$ and $[Pb(L^4)(SCN)]^+$ systems were characterized by means of density functional theory calculations (DFT) performed by using the B3LYP model, and the coordination geometry as well as the role of the Pb^{II} lone pair has been investigated and discussed.

Introduction

Lead is regarded as a serious environmental pollutant.[1] Considered as a cheap and convenient material to convey water to the consumers' tap, lead has been widely used for municipal service pipes, household plumbing, joints and solders. Other major uses also include electric storage batteries, paint pigments, gasoline additives or ammunition.[2] The awareness of its environmental and health effects has led the authorities to ban some of these uses in most of the developed countries, which has contributed to a decrease in the lead level in the environment. Even so, this level is still a high risk for health, and lead continues to be one of the ten most common pollutants. In fact, the concentration in drinking water, diets and ambient air is significant in some areas.[2–5]

The removal of toxic heavy metal contaminants from aqueous waste streams is currently one of the most important environmental issues under investigation. Precipitation, activated carbon absorption, bioremediation, reverse osmosis, electrolysis, cementation, irradiation, zeolite absorption, evaporation, membrane processes or ion flotation are some of the treatment methods used for heavy metal-containing waste remediation.[6] Solvent extraction and treatment with cation exchange resins are also important, especially when selective extractions are required and/or low concentrations of the target metal ion are present. Solvent extraction occurs when a metal ion associates with an organic complexant to form a species that is transferred from the aqueous to the organic phase in a two-phase system, whereas cation exchange resins are formed by a polymeric skeleton functionalized with a complexant agent capable of binding to the desired metal ion; therefore, these two methods require the presence of a selective complexant agent. The efficient use of Pb^{II} complexant agents capable of acting as extracting agents requires that the following conditions are met: (i) fast binding of the metal ion by the complexant agent; (ii) selective ion complexation; (iii) sufficiently high binding strength for the metal ion to be extracted; (iv) high stability against hydrolysis, and (v) reversible complexation allowing for the total recovery of the metal without significant extracting agent destruction.[7] The search for novel

[a] Dpto. Química Fundamental, Facultade de Ciencias, Campus da Zapateira s/n, Universidade da Coruña,
15071 A Coruña, Spain
Fax: +34-981-167065
E-mail: mayter@udc.es
Supporting information for this article is available on the WWW under http://www.eurjic.org or from the author.

highly selective complexant agents for Pb^{II} requires a great knowledge of the chemical behaviour of this cation, which has caused a resurgence of interest in its chemistry.[8–12] In recent years many reports concerning coordination chemistry of Pb^{II} with a great variety of receptors have been published. The Pb^{II} cation exhibits a rich and interesting coordination chemistry: it binds to a broad range of donor groups, assumes a wide range of coordination numbers and geometries and can exhibit the so-called "inert-pair effect".

Because of the highly favoured complexation, thanks to the chelate and macrocyclic effects, chelate and macrocyclic ligands have been widely used for metal extractions. Particularly, crown ethers have been recognized as a very effective class of compounds to achieve selective separation of heavy metal ions from aqueous solutions. Separation processes based on crown ether complexes of Pb^{II} have been reported and are often quite selective.[13] In particular, we are interested in the design of selective complexant agents for Pb^{II} based on crown frameworks. In a recent work[14] we have found that the macrobicyclic receptor **L⁵** (see Scheme 1), derived from 4,13-diaza-18-crown-6, incorporating a pyridinyl Schiff-base spacer, allows reversible and fast complexation of Pb^{II}. This, together with the inertia of the receptor towards hydrolysis, opens very interesting perspectives for the use of this receptor as a new lead(II) extracting agent.[15] As a continuation of this work we discuss the potential of the related receptor **L⁴** as a complexant agent for this metal ion. Likewise, the effect that the presence of different counterions and the protonation of the receptor has on the Pb^{II} coordination environment have also been investigated. Receptors **L⁴** and **L⁵** derive structurally from the bibracchial lariat ethers **L¹** and **L²**, respectively, and belong to the group defined as (Schiff base) lateral macrobicycles.[16] Although both Schiff-base macrocycles and cryptands have been proposed as excellent platforms for the complexation of a wide variety of metal ions,[17,18] no example of a Schiff-base lateral macrobicycle was reported until 1999[19] when we prepared the macrobicycles **L³**–**L⁶** (see Scheme 1). Subsequent studies have demonstrated that these systems possess very promising coordinating properties.[20–22]

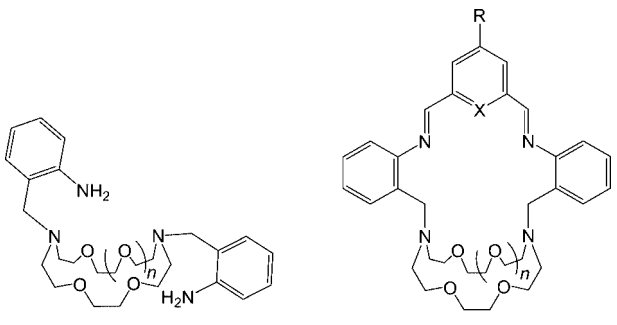

$Pb(L^4)(ClO_4)_2 \cdot 0.5\,H_2O$ (**1**) $[H_3L^4](ClO_4)_3 \cdot 3\,CH_3CN$ (**2**)

Scheme 1.

Results and Discussion

Reaction between the barium complex $[Ba(L^4)](ClO_4)_2$ and $Pb(ClO_4)_2 \cdot 6H_2O$ yields the Pb^{II} compound of formula $Pb(L^4)(ClO_4)_2 \cdot 0.5H_2O$ (**1**). The absence of peaks corresponding to species containing the $[Ba(L^4)]^+$ fragment in the FAB-mass spectrum coupled with the presence of an intense peak from $[Pb(L^4)(ClO_4)]^+$ confirmed that the macrobicycle **L⁴** remains intact and that transmetallation has occurred.

Slow diffusion of diethyl ether into a solution of **1** in acetonitrile gave X-ray quality crystals of this compound. Crystals comprise the cation $[Pb(L^4)(ClO_4)]^+$, a well-separated perchlorate group and an acetonitrile molecule. Figure 1 illustrates the structure of the complex cation, while selected bond lengths and angles of the coordination sphere are compiled in Table 1. The Pb^{II} ion is set into the macrobicyclic cavity, bound to six of the eight heteroatoms of the receptor **L⁴** and two oxygen atoms of a perchlorate group. The interaction between the Pb^{II} ion and this perchlorate group is very weak, as indicated by the $Pb–O_{perchlorate}$ distances, Pb–O(11) 2.838(5) and Pb–O(9) 3.000(7). Very often these weak interactions have been described as "semicoordination",[23] and it is usually attributed to crystal packing forces in the solid state.

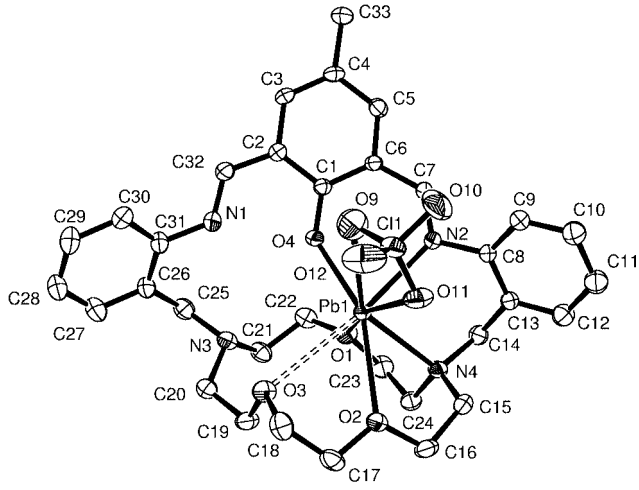

Figure 1. X-ray crystal structure of the cation in compound **1** with atom labelling; hydrogen atoms are omitted for simplicity; the ORTEP plot is drawn at the 30% probability level.

As shown in Figure 1, in $[Pb(L^4)(ClO_4)]^+$ the Pb^{II} ion is asymmetrically placed at one end of the macrobicyclic cavity, coordinated to one imine nitrogen atom, N(2), one pivotal nitrogen atom, N(4), the phenol oxygen atom, O(4), and the three oxygen atoms of the crown moiety, O(1), O(2) and O(3). The Pb^{II} ion is clearly closer to O(1) than to O(2) and O(3), and the considerably long Pb–O(3) and Pb–O(2) distances [3.117(5) and 2.844(4) Å, respectively] suggest that the interaction of Pb^{II} with these oxygen donor atoms is

Table 1. Selected bond lengths [Å] and angles [°] for **1**.

Pb–O(1)	2.556(4)	Pb–O(9)	3.000(7)
Pb–O(2)	2.844(4)	Pb–O(11)	2.838(5)
Pb–O(3)	3.117(5)	Pb–N(2)	2.537(5)
Pb–O(4)	2.379(4)	Pb–N(4)	2.588(5)
O(4)–Pb(1)–N(2)	74.51(15)	O(4)–Pb(1)–O(1)	74.82(14)
N(2)–Pb(1)–O(1)	95.29(15)	O(4)–Pb(1)–N(4)	131.15(16)
N(2)–Pb(1)–N(4)	79.29(15)	O(1)–Pb(1)–N(4)	67.35(15)
O(4)–Pb(1)–O(11)	117.73(14)	N(2)–Pb(1)–O(11)	76.25(16)
O(1)–Pb(1)–O(11)	161.21(15)	N(4)–Pb(1)–O(11)	94.38(16)
O(4)–Pb(1)–O(2)	156.31(14)	N(2)–Pb(1)–O(2)	129.14(14)
O(1)–Pb(1)–O(2)	98.75(14)	N(4)–Pb(1)–O(2)	62.23(15)
O(11)–Pb(1)–O(2)	75.03(14)	O(4)–Pb(1)–O(9)	72.11(16)
N(2)–Pb(1)–O(9)	72.64(17)	O(1)–Pb(1)–O(9)	146.73(17)
N(4)–Pb(1)–O(9)	136.21(17)	O(11)–Pb(1)–O(9)	46.96(16)
O(2)–Pb(1)–O(9)	113.02(16)	O(4)–Pb(1)–O(3)	99.15(13)
N(2)–Pb(1)–O(3)	173.36(13)	O(1)–Pb(1)–O(3)	84.78(13)
N(4)–Pb(1)–O(3)	106.76(14)	O(11)–Pb(1)–O(3)	105.58(14)
O(2)–Pb(1)–O(3)	57.26(12)	O(9)–Pb(1)–O(3)	103.76(16)

weak. The other two heteroatoms of the macrobicyclic receptor, the imine and pivotal nitrogen atoms N(1) and N(3), do not belong to the metal ion coordination environment, as evidenced by the observed Pb–N(1) and Pb–N(3) distances of 4.4515(4) and 4.0474(3) Å, respectively. Moreover, the X-ray data suggest that the imine nitrogen atom N(1) and the phenol donor O(4) are involved in an intramolecular hydrogen bonding interaction [N(1)···H(1N), 0.84(7) Å; N(1)···O(4) 2.598(7) Å, O(4)···H(1N) 1.95(8) Å, N(1)–H(1N)–O(4) 133(7)°]. These distances also indicate that proton transfer from the phenol group to the imine atom N(1) has occurred. This proton transfer has also been observed in the related complexes $[Ba(L^4)(ClO_4)(CH_3CN)]^+$[24] and $[Pb(L^6)]^{2+}$,[21] where the guest metal ion is also asymmetrically located in the macrobicyclic cavity. A remarkable characteristic of the complex is the presence of chirality induced by the asymmetric position of the metal ion inside the macrobicyclic cavity. Inspection of the crystal data reveals that in **1** both enantiomers cocrystallize in equal amounts (racemate).

The fold of $\mathbf{L^4}$ around the Pb^{II} ion allows the five donors of the crown moiety, [O(1), O(2), O(3), N(3) and N(4)], to be essentially coplanar (mean deviation from plane 0.0762 Å), with the metal ion located 1.6955 Å above this plane. The coordination polyhedron may be described as a distorted monocapped pentagonal bipyramid (Figure 2). The torsion angles C(1)–C(6)–C(7)–N(2) [–6.8(10)°] and C(1)–C(2)–C(32)–N(1) [–5.1(10)°] indicate that both imine groups are slightly rotated from coplanarity with the phenol ring. This planarity loss is related to the structure of the receptor and the coordinative requirements of the metal ion guest that force the receptor to fold increasing the stress of its structure. The lateral aromatic rings of $\mathbf{L^4}$ in **1** are in different planes and intersect at 47.08°, a value substantially different from that found in the analogous barium complex $[Ba(L^4)(ClO_4)(CH_3CN)]^+$ (57.62°).[24] Likewise, the phenol ring forms a dihedral angle of 43.48° with the plane containing the benzyl ring attached to the pivotal nitrogen atom N(4), and an angle of 48.65° with the plane containing the other aromatic ring. The former is 23.9° larger than that found in $[Ba(L^4)(ClO_4)(CH_3CN)]^+$, whereas the latter is 16.3° smaller.[24] These results highlight the ability of $\mathbf{L^4}$ to adapt its conformation to the steric and electronic requirements of the metal ion.

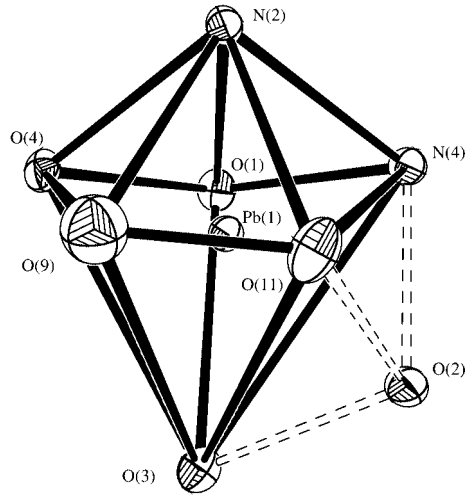

Figure 2. Coordination polyhedron around the metal ion in $[Pb(L^4)(ClO_4)]^+$.

The conductivity measurement for an ca. 10^{-3} M solution of **1** in acetonitrile at 20 °C (Λ_M = 255 $cm^2\,\Omega^{-1}\,mol^{-1}$) reveals that this compound behaves as a 2:1 electrolyte in this solvent,[25] indicating that the perchlorate anions are not coordinated to the metal ion in the acetonitrile solution. This is expected when taking into account the weak interaction of a perchlorate anion with the metal ion observed in the solid state. The ^1H NMR spectrum of **1** recorded in CD_3CN solution at 320 K is consistent with the presence of a single complex species in solution with an effective C_s symmetry (Figure 3). Upon decreasing the temperature the signals corresponding to the imine and aromatic protons gradually broaden and finally split into two different signals, reflecting intramolecular conformational exchange processes (Figure 3). The spectrum recorded at 248 K shows two resonances at δ = 8.79 and 8.75 ppm attributable to the protons of the imine units, and two signals at δ = 7.90 and 7.78 ppm with a ^4J = 2.4 Hz from the aromatic protons of the phenol group. This is consistent with the presence of a single species in solution with C_1 symmetry, in agreement with the X-ray crystal structure described above. Indeed, in the solid state the Pb^{II} ion is placed at one end of the macrobicyclic cavity, which results in a complex with C_1 symmetry. Thus, the dynamic bevaviour of compound **1** in acetonitrile solution can be attributed to a translocation of the Pb^{II} ion from one end of the macrobicyclic cavity to the other. This dynamic process is fast on the NMR timescale at high temperature, thus resulting in a spectrum corresponding to a species with an effective C_s symmetry in solution. From the coalescence temperature of signals corresponding to the aromatic protons of the phenol unit, which occurs at 309 K, we can estimate an activation barrier of $\Delta G^{\ddagger} = 68 \pm 2$ kJ mol^{-1} for this intramolecular dy-

namic process. As discussed above, the presence of the Pb^{II} ion at one end of the macrocyclic cavity in **1** induces chirality in the complex. Thus, the dynamic process observed for this compound in solution corresponds to the interconversion between the two possible enantiomeric forms of the complex.

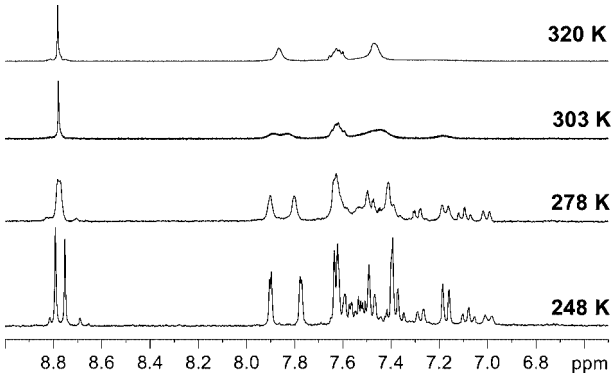

Figure 3. Part of the 300-MHz ^{1}H-NMR spectra of compound **1** recorded in CD_3CN at different temperatures.

The $[Pb(L^4)]^{2+}$ system was characterized by means of DFT calculations at the B3LYP level. On the basis of our previous experience for these calculations we used the standard 6-31G(d) basis set for the ligand atoms, while the LanL2DZ valence and effective core-potential functions were used for Pb.[26] The calculated structure for this complex (Figure 4) resembles the X-ray crystal structure of **1**, with the calculated bond lengths of the metal coordination environment in reasonable agreement with those obtained experimentally (Table 2). The experimental and calculated bond lengths differ by less than 0.08 Å, except the Pb–O(3) distance, which differs by ca. 0.18 Å from the experimental value. However, this is not surprising since the experimental value of the Pb–O(3) distance [3.117(5) Å] indicates a weak interaction between the metal ion and O(3). Shimoni-Livny et al.[27] have investigated a close relation between the role of a lone pair of Pb^{II} and the coordination geometry for a large number of Pb^{II} complexes. They have found two general structural categories of Pb^{II} compounds: holodirected and hemidirected, which are distinguished by the disposition of ligands around the metal ion. In the hemidirected form there is a void in the liganding attributable to the stereochemical activity of the Pb^{II} lone pair that is not found in holodirected geometry. The calculated Pb–O(1) bond length [2.479 Å] is clearly shorter than distances between the metal ion and the remaining oxygen atoms of the crown moiety. This, together with the presence of an identifiable void in the disposition of the donor atoms of the ligand around the metal ion, suggests that the Pb^{II} lone pair is stereochemically active in $[Pb(L^4)]^{2+}$. The analysis of the natural bond orbitals (NBO) in $[Pb(L^4)]^{2+}$ shows that the Pb^{II} lone pair orbital is predominantly 6s, but polarized by some 6p contribution: s[98.02%]p[1.98%]. Similar p contributions (>1%) have been calculated for hemidirected Pb^{II} complexes with related ligands, which clearly confirm that the Pb^{II} lone pair is stereochemically active in $[Pb(L^4)]^{2+}$.[26] However, we notice that in the X-ray crystal structure the Pb–O(1) bond length is slightly longer than the calculated one, which suggests that the presence of a weakly coordinating perchlorate anion around the Pb^{II} ion decreases the stereochemical activity of the Pb^{II} lone pair.

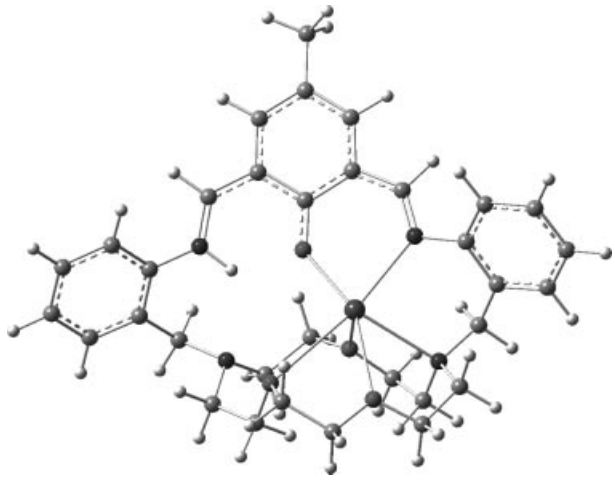

Figure 4. Structure of $[Pb(L^4)]^{2+}$ as optimized in vacuo at the B3LYP/6-31G(d) level.

Table 2. Calculated (B3LYP/6-31G(d)) bond lengths [Å] of the Pb^{II} coordination environment obtained for the $[Pb(L^4)]^{2+}$, $[Pb(L^4)(NO_3)]^+$ and $[Pb(L^4)(NCS)]^+$ systems (see Figure 1 for numbering scheme).

	$[Pb(L^4)]^{2+}$	$[Pb(L^4)(NO_3)]^+$	$[Pb(L^4)(NCS)]^+$	$[Pb(L^4)(SCN)]^+$
Pb–O(1)	2.479	2.843	2.965	2.916
Pb–O(2)	2.772	2.835	2.757	2.831
Pb–O(3)	2.935	3.191	2.862	2.916
Pb–O(4)	2.316	2.439	2.396	2.329
Pb–N(2)	2.485	2.550	2.565	2.535
Pb–N(4)	2.610	2.725	2.874	2.881
Pb–ONO_2		2.429/2.479		
Pb–NCS			2.308	
Pb–SCN				2.870

Interaction with Anions

Since in solution the Pb^{II} ion is coordinatively unsaturated in **1**, we have studied the interaction of this compound with anions such as NO_3^- and SCN^- by using spectrophotometric titrations in acetonitrile solution. The UV/Vis spectrum of **1** (Figure 5) displays a band centred at 456 nm typical of the C=N chromophores.[28,29] Upon addition of NO_3^- or SCN^- anions this band undergoes a blue shift to ca. 423 nm as its intensity decreases. Nonlinear least-squares analyses of the titration profiles (absorbance versus equivalents of anion added, see insets of Figure 5) clearly indicated the formation of 1:1 complexes in every case, and allowed us to estimate the association constants defined as [Equation (1)].

$$[Pb(L^4)]^{2+} + X^- \rightleftarrows [Pb(L^4)(X)]^+, \text{ where } X^- = NO_3^- \text{ or } SCN^- \quad (1)$$

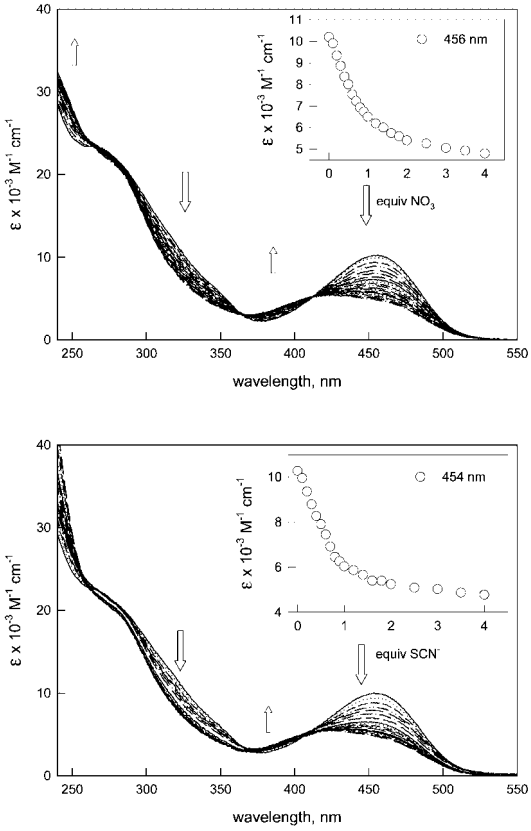

Figure 5. UV/Vis spectra taken over the course of the titration of a 10^{-5} M solution of compound **1** with a standard solution of tetrabutylammonium nitrate (top) or thiocyanate (bottom). The insets show titration profiles at selected wavelengths.

The analysis of the experimental data provides log *K* values of 5.83(1) ($X^- = NO_3^-$) and 6.27(2) ($X^- = SCN^-$). These results clearly confirm that the metal ion is coordinatively unsaturated in the Pb^{II} complex of $\mathbf{L^4}$, and indicate that the SCN^- ligand binds more strongly to $[Pb(L^4)]^{2+}$ than NO_3^-.

DFT calculations performed on the $[Pb(L^4)(NO_3)]^+$ system (see Supporting Information) indicate that the coordination of the nitrate anion has an important effect on the bond lengths of the metal coordination environment, which increase by ca. 0.06–0.36 Å with respect to those calculated for $[Pb(L^4)]^{2+}$ (Table 2). The NO_3^- ligand coordinates in a nearly symmetrical bidentate fashion [Pb–O 2.429 and 2.479 Å]. In order to understand if the coordination of the thiocyanate ligand occurs through the nitrogen atom or through the sulfur one we have also carried out DFT calculations on the $[Pb(L^4)(NCS)]^+$ and $[Pb(L^4)(SCN)]^+$ systems. Pb^{II} is classified as "intermediate" in the Pearson HSAB classification,[30] and thus it is not particularly surprising that both *N*-bonded and *S*-bonded Pb^{II} complexes of thiocyanate exist.[31] The optimized geometries for both compounds are given in the Supporting Information. Our calculations predict that the *N*-bonded thiocyanate ligand results in a more stable structure, where the in vacuo relative energy of the $[Pb(L^4)(SCN)]^+$ system with respect to the $[Pb(L^4)(NCS)]^+$ is 5.47 kcal mol^{-1}. This is in agreement with the X-ray structure of the Pb^{II} thiocyanate complex with the related macrobicycle $\mathbf{L^3}$, which shows that the thiocyanate ligand is *N*-bonded.[22] This is probably because the steric hindrance around the metal ion, caused by the coordination of the macrobicyclic receptor, favours the coordination of the SCN^- ligands through the N donor atom.[32] On the other hand, the analysis of the NBOs in $[Pb(L^4)(NO_3)]^+$ indicates that the 6p contribution decreases upon coordination of the nitrate anion: s[98.57%]p[1.43%]. As a consequence the coordination geometry in $[Pb(L^4)(NO_3)]^+$ is less hemidirected than in $[Pb(L^4)]^{2+}$, and the Pb–O(1) bond length increases (Table 3). Replacing the nitrate anion by a *N*-bonded thiocyanate ligand results in a somewhat lower polarization of the Pb 6s lone pair, as follows from the NBOs analysis: s[98.72%]p[1.28%]. Furthermore, the presence of a *S*-bonded thiocyanate ligand causes a further decrease of the polarization of the Pb 6s lone pair: s[99.28%]p[0.72%]. Thus, the polarization of the Pb lone pair decreases when hard donor atoms such as O atoms of the nitrate group are replaced by softer donor atoms such as the N or S donor atoms of a thiocyanate ligand. These results are in agreement with previous observations that indicated that the coordination of soft-donor atoms favours holodirected ligand geometries in Pb^{II} complexes.[26,27]

Table 3. ^{1}H- and ^{13}C-NMR spectroscopic data [ppm] for compound $[H_2L^4]^{2+}$ in CD_3CN solution at 298 K.[a]

H atom[b]	δ values	C atom	δ values
H1	2.41 (s, 3 H)	C1	20.1
H3	7.70 (s, 2 H)	C2	130.8
H6	8.66 (s, 2 H)	C3	140.8
H8	7.31 (d, 2 H)	C4	122.4
H9	7.60 (td, 2 H)	C5	158.4
H10	7.40 (t, 2 H)	C6	166.6
H11	7.49 (d, 2 H)	C7	151.0
H13	4.31 (d, 2 H)	C8	120.8
H13′	4.72 (d, 2 H)	C9	132.9
H14	3.43 (m, 2 H)	C10	128.6
H14′	3.43 (m, 2 H)	C11	132.7
H15	3.40 (m, 2 H)	C12	124.3
H15′	3.64 (m, 2 H)	C13	58.9
H16	2.99 (m, 2 H)	C14	55.6
H16′	3.41 (m, 2 H)	C15	64.8
H17	3.42 (m, 2 H)	C16	69.8
H17′	3.88 (m, 2 H)	C17	56.9
H18	3.78 (m, 2 H)	C18	65.1
H18′	4.01 (m, 2 H)		

[a] See Figure 6 for labelling. [b] $^3J_{8,9}$ = 7.9 Hz; $^3J_{11,10}$ = 7.4 Hz; $^4J_{9,11}$ = 1.3 Hz; $^2J_{13,13'}$ = 13.8 Hz.

Protonation Studies

The protonation of $Pb(L^4)(ClO_4)_2 \cdot 0.5H_2O$ (**1**) has been followed by NMR and UV/Vis spectroscopy in CH_3CN solutions at room temperature. Upon addition of trifluoroacetic acid to a solution of **1** in CD_3CN a new set of signals is observed in the ^{1}H NMR spectra whose chemical shifts do not vary with the amount of trifluoroacetic acid added,

thereby confirming the formation of a single protonated species in acetonitrile solution. Upon addition of two equivalents of acid the signals of compound **1** nearly disappear, in agreement with the formation of the diprotonated species $[H_2L^4]^{2+}$ (see Figure 6). The two protonations probably occur on the pivotal nitrogen atoms, as previously observed for $[H_2L^5]^{2+}$.[33] The ^1H and ^{13}C NMR spectra of $[H_2L^4]^{2+}$ could be fully assigned on the basis of two-dimensional COSY, HSQC and HMBC experiments at 298 K (Table 3, see Figure 6 for labelling). The ^{13}C NMR spectrum shows 18 signals for the 33 carbon nuclei of the ligand, indicating an effective C_s symmetry of $[H_2L^4]^{2+}$ in acetonitrile solution. The methylene protons H13/H13′ yield an AB spin pattern ($^2J_{13,13'}$ = 13.8 Hz) in the ^1H NMR spectrum, while the protons of the crown moiety give AA′BB′ spin patterns (Figure 6). This is indicative of a relatively rigid structure of $[H_2L^4]^{2+}$ in solution, probably because of the presence of intramolecular hydrogen bonding interactions between the protonated pivotal nitrogen atoms and oxygen atoms of the crown moiety.

Figure 7 shows a family of UV/Vis spectra recorded during the course of a titration of a 10^{-4} M solution of **1** with trifluoroacetic acid in CH_3CN solution. Upon addition of trifluoroacetic acid the band at 456 nm experiences a blue shift to 364 nm. The presence of two sharp isosbestic points at 394 and 335 nm indicates that only two species co-exist at the equilibrium, while the profile shown in the inset of Figure 7 indicates the formation of a diprotonated species in solution upon addition of trifluoroacetic acid. Data can be interpreted on the basis of equilibrium (2).

$$[Pb(L^4)]^{2+} + 2\ H^{+} \rightleftarrows [(H_2L^4)]^{2+} + Pb^{2+},\ \beta_{12} \qquad (2)$$

A nonlinear least-squares treatment of the titration profile provides $\log\beta_{12}$ = 9.14(1). These results confirm that addition of acid to a solution of **1** causes the demetallation of the complex together with the formation of the diprotonated form of the ligand, as previously observed for $[Pb(L^5)]^{2+}$.[14] However, in the latter case the demetallation process has been shown to occur in two steps, with the formation of an intermediate monoprotonated complex species $[Pb(HL^5)]^{3+}$. By contrast, the demetallation of $[Pb(L^4)]^{2+}$ appears to occur in a single step, as described by Equation (2).

Addition of a large excess of CF_3COOH to a solution of $[H_2L^4]^{2+}$ provokes further changes in the UV/Vis spectrum (Figure 7); the band from the imine group at 364 nm shows a red shift towards 495 nm. This result suggests that a third protonation process occurs in the presence of a large excess of acid. Slow evaporation of a solution of **1** in the presence of 10 equiv. of CF_3COOH allowed us to obtain single crystals of $[H_3L^4](ClO_4)_3{\cdot}3CH_3CN$ (**2**) suitable for single-crystal X-ray diffraction studies, which confirms the formation of the triprotonated form of the macrobicycle under these conditions. Crystals of **2** contain the cation $[H_3L^4]^{3+}$, three perchlorate anions and acetonitrile molecules. Figure 8 shows the structure of the cation in **2**. Bond lengths and angles do not show significant deviations from the expected values. The conformation of the macrobicycle in **2** is conditioned by the presence of intramolecular hydrogen bonding interactions (Table 4) involving each pivotal nitrogen atom with two oxygen atoms of the crown moiety and both imine nitrogen atoms with the oxygen atom of the phenol group. This type of interaction seems to be responsible for the relatively rigid structure found in solution for the related diprotonated receptor $[H_2L^4]^{2+}$ described above.

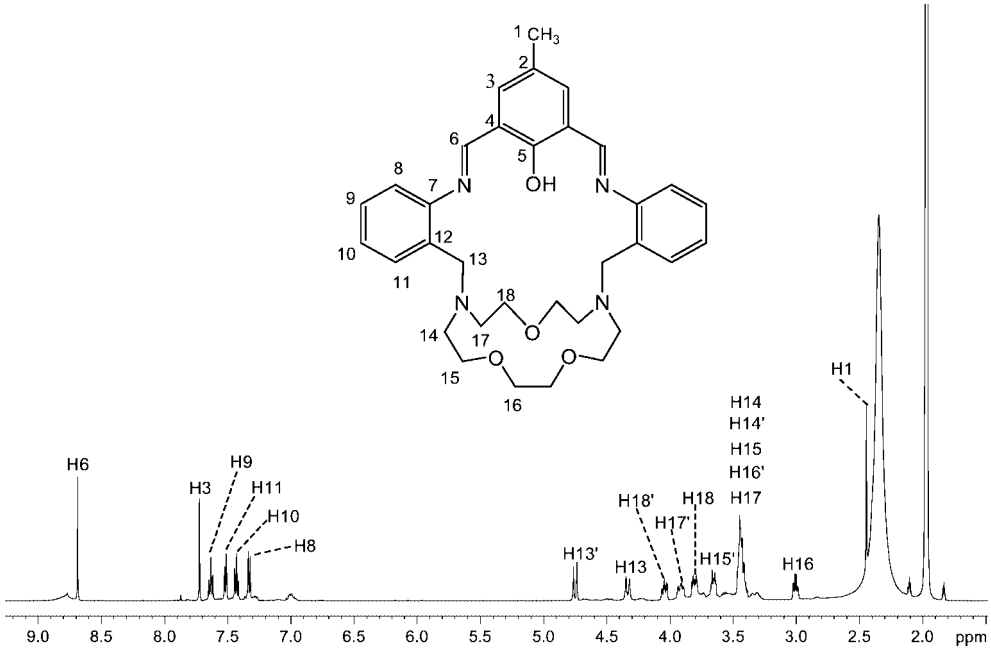

Figure 6. ^1H-NMR spectrum of $[H_2L^4]^{2+}$ recorded in CD_3CN solution at 298 K.

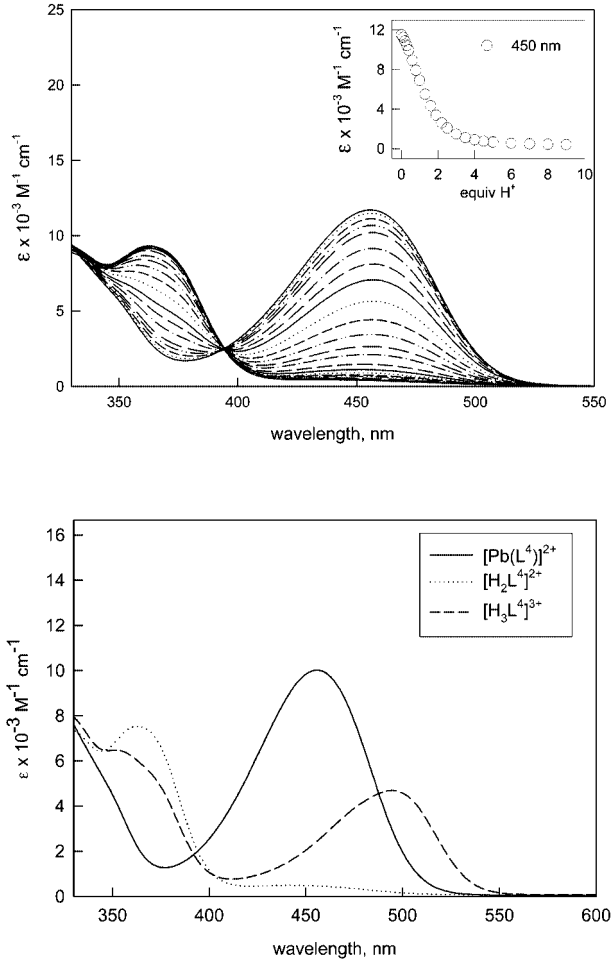

Figure 7. Top: family of spectra taken over the course of the titration of an acetonitrile solution 10^{-5} M in **1** with a standard solution of CF_3COOH at 298 K. The titration profile is reported in the inset. Bottom: comparison of the UV/Vis spectra of $[Pb(L^4)]^{2+}$, $[H_2L^4]^{2+}$ and $[H_3L^4]^{3+}$ as recorded in acetonitrile solution.

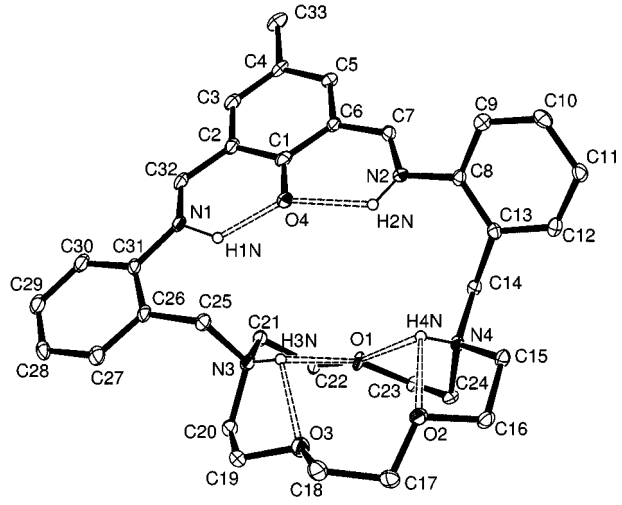

Figure 8. ORTEP diagram (30% probability) of $[H_3L^4]^{3+}$ in **2**, showing the atomic numbering scheme. For the sake of clarity hydrogen atoms are omitted, except those involved in intramolecular hydrogen bonds.

Table 4. Distances [Å] and angles [°] of intramolecular hydrogen bonds in compound **2**.[a]

D–H···A	H···A	D···A	D–H···A
N(3)–H(3N)···O(1)	2.33(6)	2.679(4)	102(4)
N(3)–H(3N)···O(3)	2.21(5)	2.714(5)	113(3)
N(4)–H(3N)···O(1)	2.49(5)	2.778(4)	100(3)
N(4)–H(3N)···O(2)	2.43(5)	2.726(6)	100(3)
N(1)–H(3N)···O(4)	1.73(5)	2.533(4)	128(4)
N(2)–H(3N)···O(4)	2.05(4)	2.656(4)	121(3)

[a] For atom labels see Figure 7.

Conclusions

The Schiff-base lateral macrobicycle **L^4**, derived from 1,10-diaza-15-crown-5 incorporating a phenol Schiff-base spacer, forms stable complexes with Pb^{II}. The X-ray crystal structure of $[Pb(L^4)(ClO_4)](ClO_4)\cdot CH_3CN$ (**1**) shows that the lead(II) ion is asymmetrically placed at the one end of the macrobicyclic cavity, because of the intramolecular hydrogen bonding interaction that occurs between an imine nitrogen atom and the phenol group. This asymmetric position of the metal ion inside the macrobicyclic cavity induces chirality in this system. The asymmetric coordination of the metal ion inside the macrocyclic cavity found in the solid state is also maintained in acetonitrile solution, but a translocation of the Pb^{II} ion from one end of the macrobicyclic cavity to the other occurs. This dynamic behaviour, which actually corresponds to the interconversion between the two possible enantiomeric forms of the complex, is fast on the NMR timescale at 320 K but slow at low temperatures, and we have estimated an activation barrier of $\Delta G^{\ddagger} = 68 \pm 2$ kJ mol^{-1}.

Both the solid state and solution structure of $[Pb(L^4)]^{2+}$ indicate that the complex is coordinatively unsaturated so that interactions with anions such as NO_3^- and SCN^- are possible. Spectrophotometric titrations in acetonitrile solution indicate that the SCN^- ligand binds more strongly to $[Pb(L^4)]^{2+}$ than NO_3^-, which follows from the values of the binding constants obtained: [$\log K = 5.83(1)$ and 6.27(2) for NO_3^- and SCN^-, respectively]. The coordination geometry as well as the role of a lone pair of Pb^{II} of the systems $[Pb(L^4)]^{2+}$, $[Pb(L^4)(NO_3)]^+$, $[Pb(L^4)(NCS)]^+$ and $[Pb(L^4)(SCN)]^+$ have been investigated by means of DFT calculations. The analysis of the natural bond orbitals (NBO) in $[Pb(L^4)]^{2+}$ shows that the Pb^{II} lone pair is stereochemically active in $[Pb(L^4)]^{2+}$. The 6p contribution decreases upon coordination of the nitrate anion, and so the coordination geometry in $[Pb(L^4)(NO_3)]^+$ is less hemidirected than in $[Pb(L^4)]^{2+}$. Replacing the nitrate anion by a *N*-bonded thiocyanate ligand results in a lower polarization of the Pb 6s lone pair, which further decreases when the SCN^- ligand is *S*-bonded. Finally, we have found that protonation of **1** with trifluoroacetic acid in acetonitrile solution causes demetallation of the complex without receptor destruction, with receptor **L^4** recovered in its protonated form. This opens interesting perspectives for the use of this receptor as a potential lead(II) extracting agent.

Experimental Section

Materials and Synthesis: $[Ba(L^4)](ClO_4)_2$ was prepared as described previously by us.[19] All other chemicals were purchased from commercial sources and used without further purification. Solvents were of reagent grade purified by the usual methods. Caution! Although we have experienced no difficulties with the perchlorate salts, these should be regarded as potentially explosive and handled with care.[34]

$Pb(L^4)(ClO_4)_2·0.5H_2O$ (1): A solution of $Pb(ClO_4)_2·6H_2O$ (0.0131 g, 0.025 mmol) in absolute ethanol (5 mL) was added while stirring to a solution of $[Ba(L^4)](ClO_4)_2$ (0.0224 g, 0.025 mmol) in the same solvent (20 mL). The reaction mixture was stirred and refluxed for 48 h. After the reaction was complete the resultant yellow solution was allowed to stand for a few days and an orange precipitate was formed, which was collected by filtration and air dried (0.016 g, 66%). $C_{33}H_{40}Cl_2N_4O_{12}Pb·0.5H_2O$ (971.2): calcd. C 40.7, H 4.2, N 5.7; found C 40.3, H 4.2, N 5.5. MS (FAB): m/z = 863 $[Pb(L^4)(ClO_4)]^+$. IR (KBr): $\tilde{\nu}$ = $(C{=}N)_{imine}$ 1633, $\nu(OH)_{phenol}$ 3470, ν_{as}(Cl–O) 1092, δ_{as}(O–Cl–O) 623 cm^{-1}. X-ray quality crystals of formula $[Pb(L^4)(ClO_4)](ClO_4)·CH_3CN$ were grown by slow diffusion of diethyl ether into a solution of **1** in acetonitrile.

Physical Methods: Elemental analyses were carried out with a Carlo–Erba 1108 elemental analyzer. FAB mass spectra were recorded using a FISONS QUATRO mass spectrometer with a Cs ion-gun and 3-nitrobenzyl alcohol as the matrix. IR spectra were recorded, as KBr discs or nujol mulls, using a Bruker Vector 22 spectrophotometer. Conductivity measurements were carried out with a Crison Micro CM 2201 conductivimeter using ca. 10^{-3} M solutions of the complex in acetonitrile. ^1H and ^{13}C NMR spectra were run at 25 °C with Bruker Avance 300-MHz or Bruker WM-500 spectrometers. Chemical shifts are reported in δ values. Spectral assignments were based in part on two-dimensional COSY, HMQC and HMBC experiments. Electronic spectra in the UV/Vis range were recorded at 20 °C with a Perkin–Elmer Lambda 900 UV/Vis spectrophotometer using 1.0 cm quartz cells. Spectrophotometric titrations were performed at 25 °C on 10^{-5} or 10^{-4} M solutions of compound **1** in acetonitrile (polarographic grade). Typically, aliquots of a fresh standard solution of the titrant salt (10^{-3} or 10^{-2} M) were added and the UV/Vis spectra of the samples were recorded. All spectrophotometric titration curves were fitted with the HYPERQUAD program.[35]

X-ray Crystallography: Crystal data and details on data collection and refinement are summarized in Table 5. Three dimensional X-ray data for $[Pb(L^4)(ClO_4)](ClO_4)·CH_3CN$ (**1**) and $[H_3L^4](ClO_4)_3·3CH_3CN$ (**2**) were collected with a Bruker Smart 1000 CCD diffractometer. Data were corrected for Lorentz and polarization effects and for absorption by semi-empirical methods. Complex scattering factors were taken from the program package SHELXTL[36] for **1**, and SHELX97[37] for **2**. Both structures were solved by direct methods and refined by full-matrix least-squares on F^2. Refinement converged with anisotropic displacement parameters for all non-hydrogen atoms. The hydrogen atoms were included in calculated positions and refined by using a riding model, except for the hydrogen atom H(1N) in **1**, and H(1N), H(2N), H(3N) and H(4N) in **2**, which were first located in a difference electron-density map and then left to freely refine. The crystal of **1** presents a disorder on the ionic perchlorate and 162 restraints had to be imposed. This disorder has been solved and two atomic sites for each oxygen atom have been observed. The site occupancy factor was 0.491 for the four oxygen atoms, O(5A), O(6A), O(7A) and O(8A). The crystal of **2** also presents disorder on one of the acetonitrile solvent molecules [site occupancy factor: 0.526 for N(7A), C(38A) and C(31A)]. CCDC-624582 and -624583 contain the supplementary crystallographic data for the structures included in this paper. These data can be obtained free of charge from The Cambridge Crystallographic Data Centre via http://www.ccdc.cam.ac.uk/datarequest/cif.

Table 5. Crystal data and refinement details for compounds **1** and **2**.

	1	**2**
Formula	$C_{35}H_{43}Cl_2N_5O_{12}Pb$	$C_{39}H_{52}Cl_3N_7O_{16}$
Mol. mass [g mol^{-1}]	1003.83	981.23
Crystal system	triclinic	monoclinic
Space group	$P\bar{1}$	$C2/c$
Temperature [K]	293(2)	100(2)
a [Å]	9.5083(9)	36.377(5)
b [Å]	13.1472(12)	13.3500(19)
c [Å]	16.2475(15)	23.350(3)
α [°]	96.506(2)	90
β [°]	101.7200	125.674(2)
γ [°]	97.083(2)	90
V [Å^3]	1953.4(3)	9212(2)
$F(000)$	1000.0	4112
Z	2	8
$\rho_{calcd.}$ [g cm^{-3}]	1.707	1.415
μ [mm^{-1}]	4.523	0.275
2θ range [°]	1.29–28.29	1.76–29.29
R_{int}	0.0432	0.1473
Measured reflections	13860	53909
Unique reflections	9472	11624
Observed reflections [$I > 2\sigma(I)$]	6929	4919
Goodness-of-fit on F^2	0.981	0.935
R_1 [$I > 2\sigma(I)$][a]	0.0440	0.0683
wR_2 (all data)[b]	0.1078	0.2023

[a] $R_1 = \Sigma||F_o| - |F_c||/\Sigma|F_o|$. [b] $wR_2 = \{\Sigma[w(|F_o|^2 - |F_c|^2)^2]/\Sigma[w(F_o^4)]\}^{1/2}$.

Computational Methods: The $[Pb(L^4)]^{2+}$, $[Pb(L^4)(NO_3)]^+$, $[Pb(L^4)(NCS)]^+$ and $[Pb(L^4)(SCN)]^+$ systems were fully optimized by using the B3LYP density functional model.[38,39] In these calculations we have used the standard 6-31G(d) basis set for the ligand atoms, while the LanL2DZ valence and effective core potential functions were used for Pb.[40] The stationary points found on the potential energy surfaces as a result of the geometry optimizations have been tested to represent energy minima rather than saddle points via frequency analysis. The relative free energy of the $[Pb(L^4)(NCS)]^+$ and $[Pb(L^4)(SCN)]^+$ complexes was calculated in vacuo at the same computational level, and it includes nonpotential energy (NPE) contributions (that is, zero point energy and thermal terms) obtained by frequency analysis. The wave functions of some of the lead complexes were analyzed by natural bond orbital analyses, involving natural atomic orbital (NAO) populations and natural bond orbitals (NBO).[41,42] All DFT calculations were performed by using the Gaussian 03 program package (Revision C.01).[43]

Supporting Information (see also the footnote on the first page of this article): Figure S1 showing B3LYP-optimized structures of the $[Pb(L^4)(NO_3)]^+$, $[Pb(L^4)(NCS)]^+$ and $[Pb(L^4)(SCN)]^+$ systems, and in-vacuo-optimized Cartesian coordinates [Å] for the $[Pb(L^4)]^{2+}$, $[Pb(L^4)(NO_3)]^+$, $[Pb(L^4)(NCS)]^+$ and $[Pb(L^4)(SCN)]^+$ systems.

Acknowledgments

The authors thank Xunta de Galicia (PGIDIT03TAM10301PR and PGIDIT06TAM10301PR) for generous financial support. The

authors are indebted to Centro de Supercomputación of Galicia (CESGA) for providing the computer facilities.

[1] R. M. Harrison, D. R. H. Laxen, *Lead Pollution*, Chapman & Hall, London, **1981**.
[2] J. M. Christensen, J. Kristiansen, in: *Handbook of Metals in Clinical and Analytical Chemistry* (Eds.: H. G. Seiler, A. Sigel, H. Sigel), Marcel Dekker, New York, **1994**, pp. 425–440.
[3] B. P. Lanphear, D. A. Burgoon, S. W. Rust, S. Eberly, W. Galke, *Environmental Res.* **1998**, *76*, 120–130.
[4] T. G. Spiro, W. M. Stigliani, *Chemistry of the Environment*, Prentice Hall, Upper Saddle River, NJ, **1996**.
[5] F. Cuenot, M. Meyer, A. Bucaille, R. Guilard, *J. Mol. Liquids* **2005**, *118*, 89–99.
[6] A. T. Yordanov, D. M. Roundhill, *Coord. Chem. Rev.* **1998**, *170*, 93–124.
[7] A. Deratani, B. Sebille, *Anal. Chem.* **1981**, *53*, 1742–1746.
[8] J. Parr, *Polyhedron* **1997**, *16*, 551–566.
[9] C. E. Holloway, M. Melnik, *Main Group Met. Chem.* **1997**, *20*, 107–132.
[10] C. E. Holloway, M. Melnik, *Main Group Met. Chem.* **1997**, *20*, 399–495.
[11] C. E. Holloway, M. Melnik, *Main Group Met. Chem.* **1997**, *20*, 583–625.
[12] E. Claudio, E. S. Godwin, H. A. Magyar, *Prog. Inorg. Chem.* **2003**, *51*, 1–144.
[13] See for instance: a) M. P. Biehl, R. M. Izatt, J. D. Lamb, J. J. Christensen, *Sep. Sci. Technol.* **1982**, *17*, 289–294; b) R. M. Izatt, G. A. Clark, J. J. Christensen, *Sep. Sci. Technol.* **1986**, *21*, 865–872; c) R. M. Izatt, R. L. Bruening, G. A. Clark, J. D. Lamb, J. J. Christensen, *Sep. Sci. Technol.* **1987**, *22*, 661–675.
[14] D. Esteban-Gómez, R. Ferreirós, S. Fernández-Martínez, F. Avecilla, C. Platas-Iglesias, A. de Blas, T. Rodríguez-Blas, *Inorg. Chem.* **2005**, *44*, 5428–5436.
[15] *Spanish patent* 2233187 B1, A. de Blas, T. Rodríguez-Blas, F. Avecilla, C. Platas-Iglesias, D. Esteban-Gómez.
[16] J.-M. Lehn, *Pure Appl. Chem.* **1980**, *52*, 2441–2459.
[17] a) C. Platas, F. Avecilla, A. de Blas, T. Rodriguez-Blas, J.-C.-G. Bünzli, *J. Chem. Soc., Dalton Trans.* **1999**, 1763–1772; b) R. Rodriguez-Cortiñas, F. Avecilla, C. Platas-Iglesias, D. Imbert, J.-C. G. Bünzli, A. de Blas, T. Rodriguez-Blas, *Inorg. Chem.* **2002**, *41*, 5336–5349.
[18] W. Radecka-Paryzek, V. Patroniak, J. Lisowski, *Coord. Chem. Rev.* **2005**, *249*, 2156–2175.
[19] D. Esteban, D. Bañobre, R. Bastida, A. de Blas, A. Macías, A. Rodríguez, T. Rodríguez-Blas, D. E. Fenton, H. Adams, J. Mahía, *Inorg. Chem.* **1999**, *38*, 1937–1944.
[20] D. Esteban, D. Bañobre, A. de Blas, T. Rodríguez-Blas, R. Bastida, A. Macías, A. Rodríguez, D. E. Fenton, H. Adams, J. Mahía, *Eur. J. Inorg. Chem.* **2000**, 1445–1456.
[21] D. Esteban, F. Avecilla, C. Platas-Iglesias, J. Mahía, A. de Blas, T. Rodríguez-Blas, *Inorg. Chem.* **2002**, *41*, 4337–4347.
[22] D. Esteban, F. Avecilla, C. Platas-Iglesias, A. de Blas, T. Rodríguez-Blas, *Polyhedron* **2003**, *22*, 2709–2717.
[23] M. N. Gowda, S. B. Naikar, G. K. Reddy, *Adv. Inorg. Radiochem.* **1984**, *28*, 255–299.
[24] F. Avecilla, D. Esteban, C. Platas-Iglesias, A. de Blas, T. Rodríguez-Blas, *Acta Crystallogr., Sect. C* **2003**, *59*, m93–m94.
[25] W. J. Geary, *Coord. Chem. Rev.* **1971**, *7*, 81–122.
[26] D. Esteban, C. Platas-Iglesias, T. Enríquez-Pérez, F. Avecilla, A. de Blas, T. Rodríguez-Blas, *Inorg. Chem.* **2006**, *45*, 5407–5416.
[27] L. Shimoni-Livny, J. P. Glusker, C. W. Bock, *Inorg. Chem.* **1998**, *37*, 1853–1867.
[28] C. Platas, F. Avecilla, A. de Blas, T. Rodríguez-Blas, C. F. G. C. Geraldes, É. Tóth, A. E. Merbach, J.-C. G. Bünzli, *J. Chem. Soc., Dalton Trans.* **2000**, 611–618.
[29] M. González-Lorenzo, C. Platas-Iglesias, F. Avecilla, S. Faulkner, S. J. A. Pope, A. de Blas, T. Rodríguez-Blas, *Inorg. Chem.* **2005**, *44*, 4254–4262.
[30] R. G. Pearson, R. Mawby, *J. Halogen Chem.* **1967**, *3*, 55–84.
[31] C. Platas-Iglesias, D. Esteban-Gómez, T. Enríquez-Pérez, F. Avecilla, A. de Blas, T. Rodríguez-Blas, *Inorg. Chem.* **2005**, *44*, 2224–2233.
[32] B. Metz, R. Weiss, *Inorg. Chem.* **1974**, *13*, 2094–2098.
[33] F. Avecilla, D. Esteban, C. Platas-Iglesias, S. Fernández-Martínez, A. de Blas, T. Rodríguez-Blas, *Acta Crystallogr., Sect. C* **2005**, *61*, o92–o94.
[34] W. C. Wolsey, *J. Chem. Educ.* **1973**, *50*, A335–A337.
[35] P. Gans, A. Sabatini, A. Vacca, *Talanta* **1996**, *43*, 1739–1753.
[36] G. M. Sheldrick, *SHELXTL Bruker Analytical X-ray System*, release 5.1, Madison, WI, **1997**.
[37] *SHELX97* [Includes *SHELXS97*, *SHELXL97*, *CIFTAB*] - Programs for Crystal Structure Analysis (Release 97-2). G. M. Sheldrick, Institut für Anorganische Chemie der Universität, Tammanstrasse 4, 37077 Göttingen, Germany, **1998**.
[38] A. D. Becke, *J. Chem. Phys.* **1993**, *98*, 5648–5652.
[39] C. Lee, W. Yang, R. G. Parr, *Phys. Rev. B* **1988**, *37*, 785–789.
[40] P. J. Hay, W. R. Wadt, *J. Chem. Phys.* **1985**, *82*, 284–298.
[41] E. D. Glendening, A. E. Reed, J. E. Carpenter, F. Weinhold, *NBO version 3.1*.
[42] A. E. Reed, L. A. Curtiss, F. Weinhold, *Chem. Rev.* **1988**, *88*, 899–926.
[43] M. J. Frisch, G. W. Trucks, H. B. Schlegel, G. E. Scuseria, M. A. Robb, J. R. Cheeseman, J. A. Montgomery Jr, T. Vreven, K. N. Kudin, J. C. Burant, J. M. Millam, S. S. Iyengar, J. Tomasi, V. Barone, B. Mennucci, M. Cossi, G. Scalmani, N. Rega, G. A. Petersson, H. Nakatsuji, M. Hada, M. Ehara, K. Toyota, R. Fukuda, J. Hasegawa, M. Ishida, T. Nakajima, Y. Honda, O. Kitao, H. Nakai, M. Klene, X. Li, J. E. Knox, H. P. Hratchian, J. B. Cross, C. Adamo, J. Jaramillo, R. Gomperts, R. E. Stratmann, O. Yazyev, A. J. Austin, R. Cammi, C. Pomelli, J. W. Ochterski, P. Y. Ayala, K. Morokuma, G. A. Voth, P. Salvador, J. J. Dannenberg, V. G. Zakrzewski, S. Dapprich, A. D. Daniels, M. C. Strain, O. Farkas, D. K. Malick, A. D. Rabuck, K. Raghavachari, J. B. Foresman, J. V. Ortiz, Q. Cui, A. G. Baboul, S. Clifford, J. Cioslowski, B. B. Stefanov, G. Liu, A. Liashenko, P. Piskorz, I. Komaromi, R. L. Martin, D. J. Fox, T. Keith, M. A. Al-Laham, C. Y. Peng, A. Nanayakkara, M. Challacombe, P. M. W. Gill, B. Johnson, W. Chen, M. W. Wong, C. Gonzalez, J. A. Pople, *Gaussian*, Inc., Wallingford CT, **2004**.

Received: October 24, 2006
Published Online: January 19, 2007

